

NACA RM L52K28

7390



TECH LIBRARY KAFB, NM
DL44345

RESEARCH MEMORANDUM

HINGE-MOMENT CHARACTERISTICS FOR SEVERAL TIP CONTROLS
ON A 60° SWEPTBACK DELTA WING AT MACH NUMBER 1.61

By K. R. Czarnecki and Douglas R. Lord

Langley Aeronautical Laboratory

Classified as Unclassified (or ~~Langley Field, Va.~~ Unclassified)

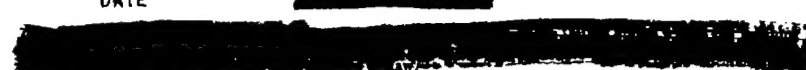
By Author: *Nasa Tech Pub Announcement #122*
(OFFICER AUTHORIZED TO CHANGE)

By..... *3 Dec 57*

..... *JK*

GRADE OF OFFICER MAKING CHANGE)

27 Mar 61
DATE



NATIONAL ADVISORY COMMITTEE
FOR AERONAUTICS

WASHINGTON
January 22, 1953

RECEIPT SIGNATURE
REQUIRED

319.98/39





NATIONAL ADVISORY COMMITTEE FOR AERONAUTICS

RESEARCH MEMORANDUM

HINGE-MOMENT CHARACTERISTICS FOR SEVERAL TIP CONTROLS

ON A 60° SWEEPBACK DELTA WING AT MACH NUMBER 1.61

By K. R. Czarnecki and Douglas R. Lord

SUMMARY

An investigation has been made at a Mach number of 1.61 and a Reynolds number of 4.2×10^6 to determine the hinge-moment characteristics of seven tip controls on a 60° sweptback delta wing. Tests were made over an angle-of-attack range from 0° to 15° and a control deflection range from -30° to 30°.

The results indicate that the most important parameter in designing delta-wing tip controls for low hinge-moment coefficients is the ratio of control-surface area ahead of the hinge line to total control-surface area. Changes in control plan form or partial shielding of the balance area have only secondary effects. Closely balanced controls tend to have more nonlinear variations of hinge-moment coefficient with control deflection than do controls having less balance area. Closely balanced controls also have a tendency to overbalance at negative control deflections at high wing angles of attack. Linear theory predicts about a 5 percent greater balance-area to total-control-area ratio required to balance the control hinge moment than is required experimentally.

INTRODUCTION

At transonic and low supersonic speeds, the hinge moments on unbalanced control surfaces become extremely large because of the large increase in the dynamic pressure. A tendency has also been observed for some trailing-edge control surfaces to exhibit losses and reversals in effectiveness at transonic speeds. One means of combatting these difficulties is the use of tip control surfaces. With a tip control surface, the hinge line may be located at any position along the root chord of the control so that the load on the control area ahead of the hinge line helps to deflect the control and thus reduce the hinge moment. The tip control is also less subject to losses and reversals in effectiveness than is the trailing-edge control.

Free-flight and wind-tunnel tests (refs. 1 and 2) have indicated that tip control surfaces provide satisfactory rolling effectiveness throughout the transonic and low supersonic speed ranges. Other free-flight tests (ref. 3) have shown that the hinge-line location on tip controls may be chosen to balance the hinge moments.

As part of a general investigation of controls, a research program is under way in the Langley 4- by 4-foot supersonic pressure tunnel to determine the important parameters in the design of controls for use on a delta wing at supersonic speeds. The results included in this report are those for a series of interchangeable tip controls tested on a 60° delta wing to determine the effect of control plan form and hinge-line location on hinge-moment characteristics at $M = 1.61$. The hinge moments were measured directly by means of strain gages and control effectiveness by means of pressure distributions. The controls were investigated over a wing angle-of-attack range from 0° to 12° or 15° and over a range of control deflections, relative to the wing, from -30° to 30° . The test Reynolds number, based on the wing mean aerodynamic chord of 12.10 inches, was 4.2×10^6 .

In order to expedite the publication of the results, only control hinge-moment characteristics will be presented in this paper, because much time is required for the reduction of the pressure data.

SYMBOLS

M	Mach number
R	Reynolds number of wing, based on wing mean aerodynamic chord
q	dynamic pressure
α	wing angle of attack
δ	control deflection relative to wing (positive when trailing edge is deflected down)
δ_t	total control deflection for two controls deflected as ailerons
S	control plan-form area
S_p	control plan-form area ahead of hinge line
\bar{c}	control mean aerodynamic chord
H	control hinge moment about hinge line

C_h control hinge-moment coefficient, $H/qS\bar{c}$

C_{h_a} net hinge-moment coefficient for two controls deflected as ailerons

$$C_{h_\alpha} = \left(\frac{\partial C_h}{\partial \alpha} \right) \text{ at } \alpha = 0^\circ, \delta = 0^\circ$$

$$C_{h_\delta} = \left(\frac{\partial C_h}{\partial \delta} \right) \text{ at } \delta = 0^\circ, \alpha = 0^\circ$$

APPARATUS

Wind Tunnel

This investigation was conducted in the Langley 4- by 4-foot supersonic pressure tunnel which is a rectangular, closed-throat, single-return type of wind tunnel with provisions for the control of the pressure, temperature, and humidity of the enclosed air. Changes in test-section Mach number are obtained by deflecting the top and bottom walls of the supersonic nozzle against fixed interchangeable templates which have been designed to produce uniform flow in the test section. The tunnel operating range is from about $1/8$ to $2\frac{1}{4}$ atmospheres stagnation pressure over a nominal Mach number range from 1.2 to 2.2.

For the tests reported herein, the nozzle walls were set for a Mach number of 1.6. At this Mach number, the test section has a width of 4.5 feet and a height of 4.4 feet. During the tests, the stagnation pressure was held at 15 pounds per square inch absolute and the dew point was kept below -20°F so that the effects of water condensation in the supersonic nozzle were negligible.

Model and Model Mounting

The model used in this investigation consisted of a half-delta wing having seven interchangeable control surfaces and various associated control adapters (or replacement sections) required to fit the controls to the basic wing. A sketch of the basic wing and seven control configurations is shown in figure 1 with the shaded area denoting the movable control surface. A photograph of the wing and control configurations, with the controls located in approximately the same relationship as in figure 1, is presented as figure 2.

The basic wing had a 60° sweptback leading edge, a root chord of 18.143 inches, and a semispan of 10.475 inches. The wing had a blunt NACA 63-series nose section extending 30 percent root chord back from the leading edge, a constant-thickness center section with a thickness ratio of 3 percent based on the root chord, and a sharp trailing edge. Near the wing tip, the nose section joined directly to the tapered trailing edge without any flat midsection. Control configurations A, B, C, and G had the same hinge-line locations, but different plan forms ahead of the hinge line, and different amounts of aerodynamic balancing area. Configurations E, F, and G had the same plan form, but different hinge-line locations and, hence, different amounts of aerodynamic balance. Configurations D and E were alike except for the removal of a portion of the control area rearward of the hinge line on configuration D. The same control adapter was used for configurations D, E, F, and G. (See fig. 2.)

The basic wing and some of the controls were of steel core construction with bismuth-tin alloy surfaces faired to the desired contours over the pressure-tube installations. The remaining control configurations and adapters were steel with the pressure-tube installations made in grooves in the surface which were faired over with a plastic material. The latter method of construction was the more satisfactory, the surface being smoother and the pressure-tube installation more reliable. All screw holes, pits, and mating lines were filled with dental plaster and faired smooth. The gap at the wing-flap parting line was maintained at approximately $\frac{1}{64}$ - inch.

The semispan control wing was mounted horizontally in the tunnel from a turntable in a steel boundary-layer bypass plate which was located vertically in the test section about 10 inches from the side wall as shown in figures 3 and 4. The bypass plate was instrumented with 60 orifices on the stream surface of the plate so that the characteristics of the flow over the plate could be established prior to and during testing of the controls.

TECHNIQUES AND TESTS

The model angle of attack was changed by rotating the turntables in the bypass plate and in the tunnel wall in which the wing and wing root were mounted. (See fig. 3.) The angle of attack was measured by a vernier on the outside of the tunnel, inasmuch as the angular deflection of the wing under load was negligible. Control deflection was changed by a gear mechanism mounted on the pressure box which rotated the strain-gage balance, the torque tube, and the control as a unit. The control angles were set approximately with the aid of an electrical control-position

indicator mounted on the torque tube close to the wing root and measured under load during testing with a cathetometer mounted outside the tunnel.

Control hinge moments were determined by means of an electrical strain-gage balance located in the pressure box (fig. 3) which measured the torque on the tube actuating the control surface. Interchangeable strain-gage beams having various load ranges were used to obtain greater accuracy for the closely balanced controls. During some of the tests, when the controls were heavily loaded, friction difficulties were experienced in the hinge-moment measuring apparatus. The friction evidenced itself as a form of hysteresis in the hinge-moment curves when data were obtained by approaching the same control settings from opposite directions. Checks for hysteresis were made throughout the tests, and whenever friction was manifest, check points were obtained by approaching control settings from both directions and friction effects eliminated by averaging the two curves. For some of the configurations, it was possible to reverse the wing and flap angles and obtain data in a region of negligible friction as a check. The results thus obtained were in very good agreement with the average or friction-corrected curves.

Tests were made over an angle-of-attack range from 0° to 12° or 15° , at increments of either 3° or 6° . The control-deflection range was from -30° to 30° , usually in increments of about 5° . The tests were made at a tunnel stagnation pressure of 15 pounds per square inch corresponding to a Reynolds number, based on the mean aerodynamic chord of 12.10 inches, of 4.2×10^6 .

PRECISION OF DATA

Calibrations made without a model indicate that the local Mach numbers over the stream surface of the plate in the region occupied by the model are within ± 0.02 of the average stream Mach number of 1.61. Flow angularities are less than 0.1° . The estimated accuracy of other pertinent quantities is

α	$\pm 0.05^\circ$
δ	$\pm 0.1^\circ$
C_h (corrected for friction)	± 0.005

RESULTS AND DISCUSSION

Hinge Moments

The variation of hinge-moment coefficient with control deflection for the various control configurations is presented in figure 5. It should be pointed out that the vertical scale for the curves of configuration A (fig. 5(a)) is 2.5 times the scale for the remaining control configurations, configuration A having much larger hinge-moment coefficients since it was the only control having no balance area ahead of the hinge line.

The general trend for all of the curves, except those for configuration G, is a statically stable or underbalanced variation, that is, a negative increase in hinge-moment coefficient for a positive increase in control deflection. Configuration G is the only control tested which was generally overbalanced for the range of α and δ of the test.

At 0° angle of attack, the variation of hinge-moment coefficient with control deflection tends to be fairly linear for each of the seven tip controls. As the angle of attack is increased, the variation of hinge-moment coefficient with control deflection becomes increasingly nonlinear. For the critically balanced controls, the hinge-moment-coefficient response becomes overbalanced for certain conditions, such as at negative control deflections for configurations D and F (figs. 5(d) and 5(f)). These regions of instability are probably a result of small movements of the center of pressure of the control lift force.

The unstable variation of hinge-moment coefficient with negative control deflection at high angles of attack, as exhibited by some of the configurations, lies in a region of special interest if the control is to be used as an elevator. An analysis of all the configurations indicates a possibility that the problem of unstable hinge moments may become more acute at values of α higher than those attained in this investigation. If tip controls are to be used as ailerons, however, the unstable variations of hinge-moment coefficients for a single control usually pose less of a problem because the combined hinge-moment coefficients of two ailerons deflected in opposite directions may be considerably more stable and in some instances the instability may be entirely eliminated. Both cases are illustrated in figure 6 where the results for configurations D and F, which show some unstable hinge-moment-coefficient variations, are presented to indicate the combined hinge-moment coefficients of an oppositely deflected pair of ailerons. Aileron configuration F shows only a small amount of instability at the high angle of attack ($\alpha = 12^\circ$) and aileron configuration D shows a completely stable variation of hinge-moment coefficient with δ at all values of α .

The variation of hinge-moment coefficient with angle of attack at constant control deflection is presented in figure 7 for the seven tip control configurations. Here again the vertical scale for configuration A is 2.5 times that for the other configurations. (It should be noted that for configurations investigated at only three values of α , the fairing of the curves may be somewhat qualitative.)

Figure 7 shows that for configurations A to F, the curves for the positive control deflections tend to have the same slopes; whereas the curves for negative control deflections tend to converge and sometimes cross over as a result of the regions of overbalance with control deflection previously discussed. On control configuration G, which was overbalanced throughout the range, the curves tend to have the same slopes for negative control deflections; whereas the curves for positive control deflections tend to converge with increasing angle of attack.

Slope Parameters

The slopes of the experimental and theoretical hinge-moment-coefficient curves are presented in figure 8 as a function of the ratio of balance area or control-surface area ahead of the hinge line to total control area. The experimental slope values were obtained from the curves of figures 5 and 7 at 0° control deflection and 0° angle of attack. The theoretical slopes were obtained by the linear-theory methods used in references 4 and 5.

From the plots, it can be seen that $C_{h\delta}$ and $C_{h\alpha}$ usually fall on straight lines both experimentally and theoretically, thus indicating a reasonable correlation on the basis of balance-area to total-control-surface-area ratio. The linear theory always predicts more negative values of hinge-moment-coefficient slopes than those found experimentally and, as a result, the theoretical prediction for the percent control area ahead of the hinge line necessary for a balanced control is about 5 percent greater than that shown to be required by experiment. Attempts to improve the correlations by taking into account the moment of the balance areas and areas rearward of the hinge line were unsuccessful as were the attempts to find other suitable parameters. In general, the second-order effects of plan form, which are indicated by the scatter of the experimental points about the experimental correlation curve, are predicted quite well by the direction and amount of scatter of the theoretical points about the theoretical correlation curve.

An idea of the magnitude of some of the secondary effects of changes in plan form or hinge-line location can easily be obtained. A comparison of the slopes $C_{h\delta}$ and $C_{h\alpha}$ for configurations B and C, for example, shows the effect of changing the plan form of the balance area. The area

rearward of the hinge line in these two controls was the same, but control C, having a greater moment area on its slightly smaller balance area, tends to give less negative (more closely balanced) values of $C_{h\alpha}$ and $C_{h\delta}$ than does control B. A part of this difference in balance effectiveness may also be ascribed to the partial shielding of the balance on configuration B. No unusual effects due to moving the hinge line without changing the plan form can be discerned. In general, it may be concluded on the basis of these results that the most important single parameter in determining the hinge-moment characteristics of tip controls on delta wings is the ratio of balance area to total control-surface area while changes in plan form and partial shielding of the balance area will (within the limits of the configurations investigated here) have only secondary effects.

Experimental values of $C_{h\delta}$ and $C_{h\alpha}$ from the tests of reference 6 are shown in figure 8. These points were obtained from a tip control having a plan form similar to configuration F, but having a slightly more rearward hinge-line location. It can be seen that these points, which were obtained in the Langley 9- by 12-inch supersonic blowdown tunnel at Mach number 1.62, are in excellent agreement with the correlation determined herein. An analysis of hinge-moment data obtained on 60° delta wings in free-flight tests at somewhat lower Mach numbers (refs. 3, 7, and 8) indicates good agreement with the present results if the data are extrapolated to the proper Mach number.

Optimum Hinge-Line Location

From the curves presented in figures 5 to 8, it is possible to estimate the optimum hinge-line location for a tip control on a 60° delta wing at $M = 1.61$. In order to provide small but stable variations of hinge-moment coefficient with control deflection and angle of attack, the hinge line may be placed to give a ratio of balance area to total control-surface area of as much as 0.35 if the control is to be used as an aileron. If the control is to be used as an elevator, then the ratio must be reduced to about 0.30 to preserve stable hinge-moment variation at negative control deflection at high angles of attack. If more linear hinge-moment-coefficient characteristics are desired than provided by those hinge-line locations, then the balance areas must be still further reduced. Possibly the linearity in hinge-moment-coefficient variation with control deflection can be improved for the closely balanced controls by the use of chordwise fences at the wing-control parting line. Such a linearizing effect has been found in the tests of reference 7.

CONCLUSIONS

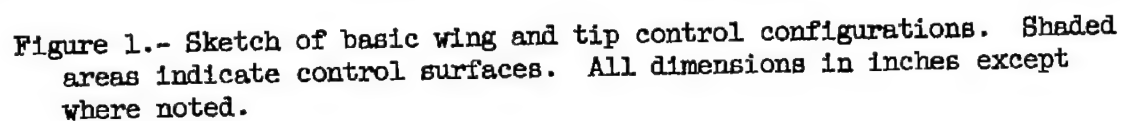
An investigation has been made to determine the hinge-moment characteristics for seven tip controls on a 60° sweptback delta wing over an angle-of-attack range from 0° to 15° and a control deflection range from -30° to 30° . Analysis of the results of these tests, which were conducted at a Mach number of 1.61 and at a Reynolds number of 4.2×10^6 , indicated that:

1. The most important parameter in designing tip controls having low hinge-moment coefficients is the ratio of control area ahead of the hinge line to the total control area. Changes in control plan form or partial shielding of the balance have only secondary effects.
2. Closely balanced controls tend to have more nonlinear variations of hinge-moment coefficient with control deflection than do controls having less balance area. Closely balanced controls also have a tendency to overbalance at negative control deflections at high wing angles of attack.
3. Linear theory predicts that 5 percent more of the total control area must be ahead of the hinge line to balance the control hinge moment than is required experimentally.
4. Approximately 5 percent more of the total control-surface area can be used for balancing purposes if the tip controls are to be used as ailerons than if they are to be used as elevators if a stable variation in the hinge-moment slope with control deflection must be maintained.

Langley Aeronautical Laboratory,
National Advisory Committee for Aeronautics,
Langley Field, Va.

REFERENCES

1. Sandahl, Carl A., and Strass, H. Kurt: Comparative Tests of the Rolling Effectiveness of Constant-Chord, Full-Delta, and Half-Delta Ailerons on Delta Wings at Transonic and Supersonic Speeds. NACA RM L9J26, 1949.
2. Conner, D. William, and May, Ellery B., Jr.: Control Effectiveness Load and Hinge-Moment Characteristics of a Tip Control Surface on a Delta Wing at a Mach Number of 1.9. NACA RM L9H05, 1949.
3. Martz, C. William, Church, James D., and Goslee, John W.: Free-Flight Investigation To Determine Force and Hinge-Moment Characteristics at Zero Angle of Attack of a 60° Sweptback Half-Delta Tip Control on a 60° Sweptback Delta Wing at Mach Numbers Between 0.68 and 1.44. NACA RM L51I14, 1951.
4. Lagerstrom, P. A., and Graham, Martha E.: Linearized Theory of Supersonic Control Surfaces. Jour. Aero. Sci., vol. 16, no. 1, Jan. 1949, pp. 31-34.
5. Tucker, Warren A., and Nelson, Robert L.: Theoretical Characteristics in Supersonic Flow of Two Types of Control Surfaces on Triangular Wings. NACA Rep. 939, 1949. (Supersedes NACA TN'S 1600, 1601, and 1660.)
6. Guy, Lawrence D.: Control Hinge-Moment and Effectiveness Characteristics of a 60° Half-Delta Tip Control on a 60° Delta Wing at Mach Numbers of 1.41 and 1.96. NACA RM L52H13, 1952.
7. Martz, C. William, and Church, James D.: Flight Investigation at Subsonic, Transonic, and Supersonic Velocities of the Hinge-Moment Characteristics, Lateral-Control Effectiveness, and Wing Damping in Roll of a 60° Sweptback Delta Wing With Half-Delta Tip Ailerons (Revised). NACA RM L51G18, 1951.
8. Martz, C. William, Church, James D., and Goslee, John W.: Rocket-Model Investigation To Determine the Force and Hinge-Moment Characteristics of a Half-Delta Tip Control on a 59° Sweptback Delta Wing Between Mach Numbers of 0.55 and 1.43. NACA RM L52H06, 1952.



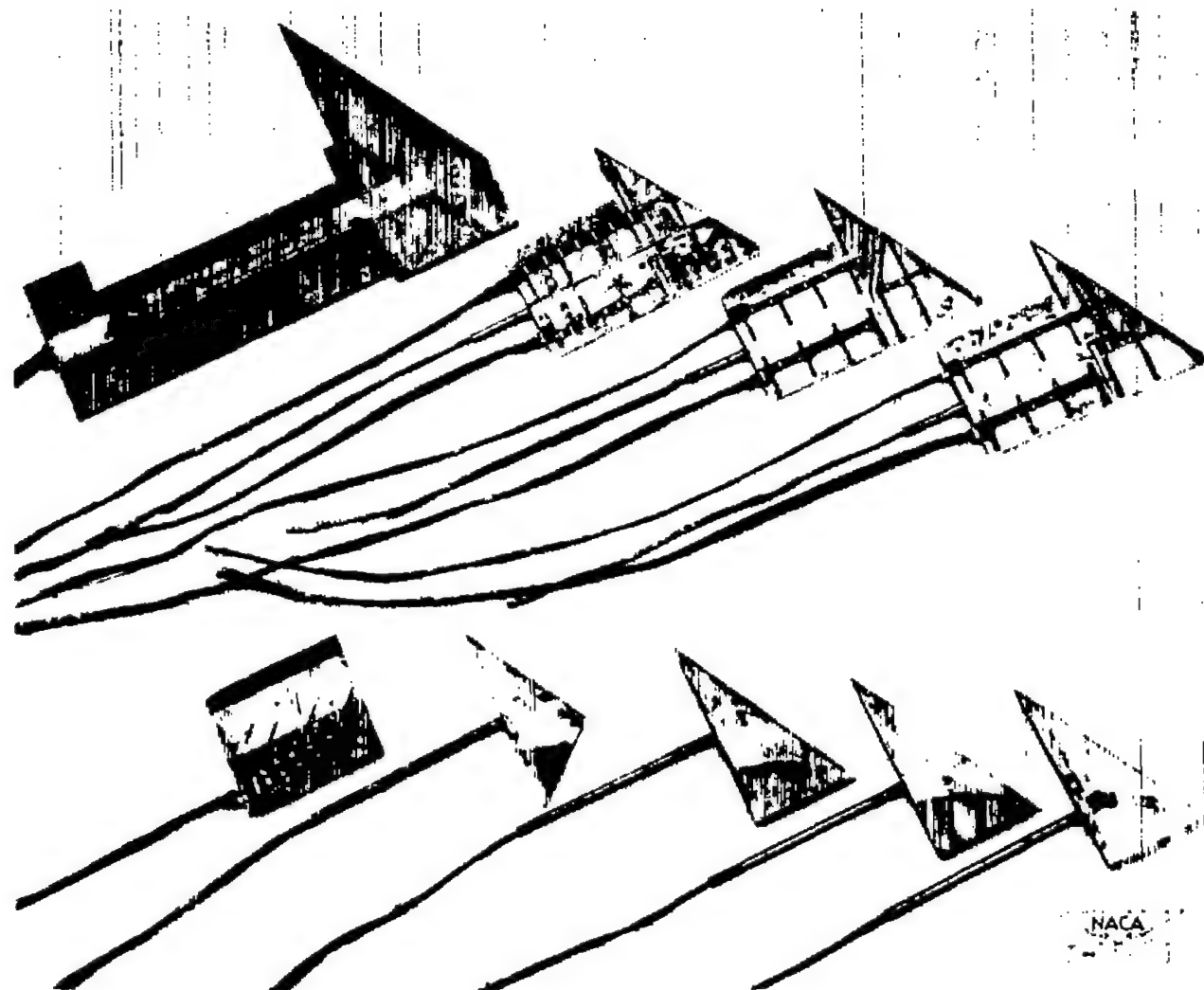


Figure 2.- Disassembled wing model and tip flaps.

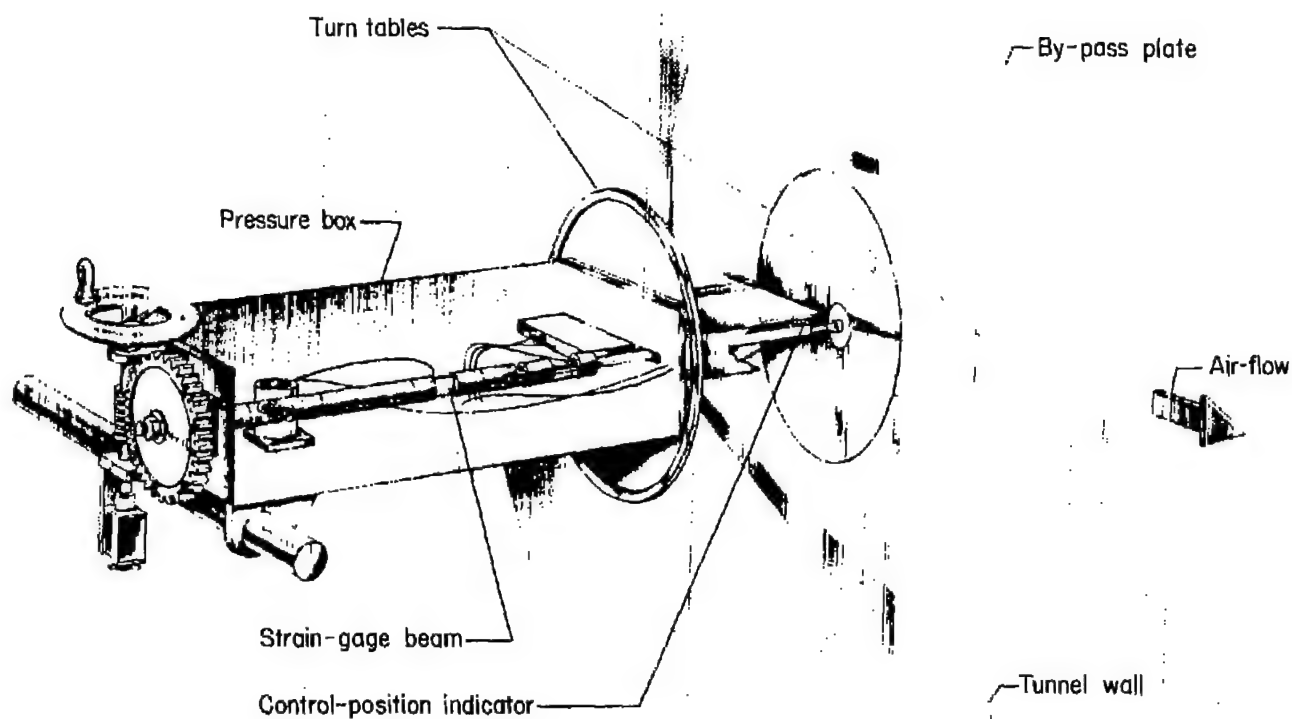


Figure 3.- Sketch of test setup to investigate hinge moments of tip controls on a delta wing.

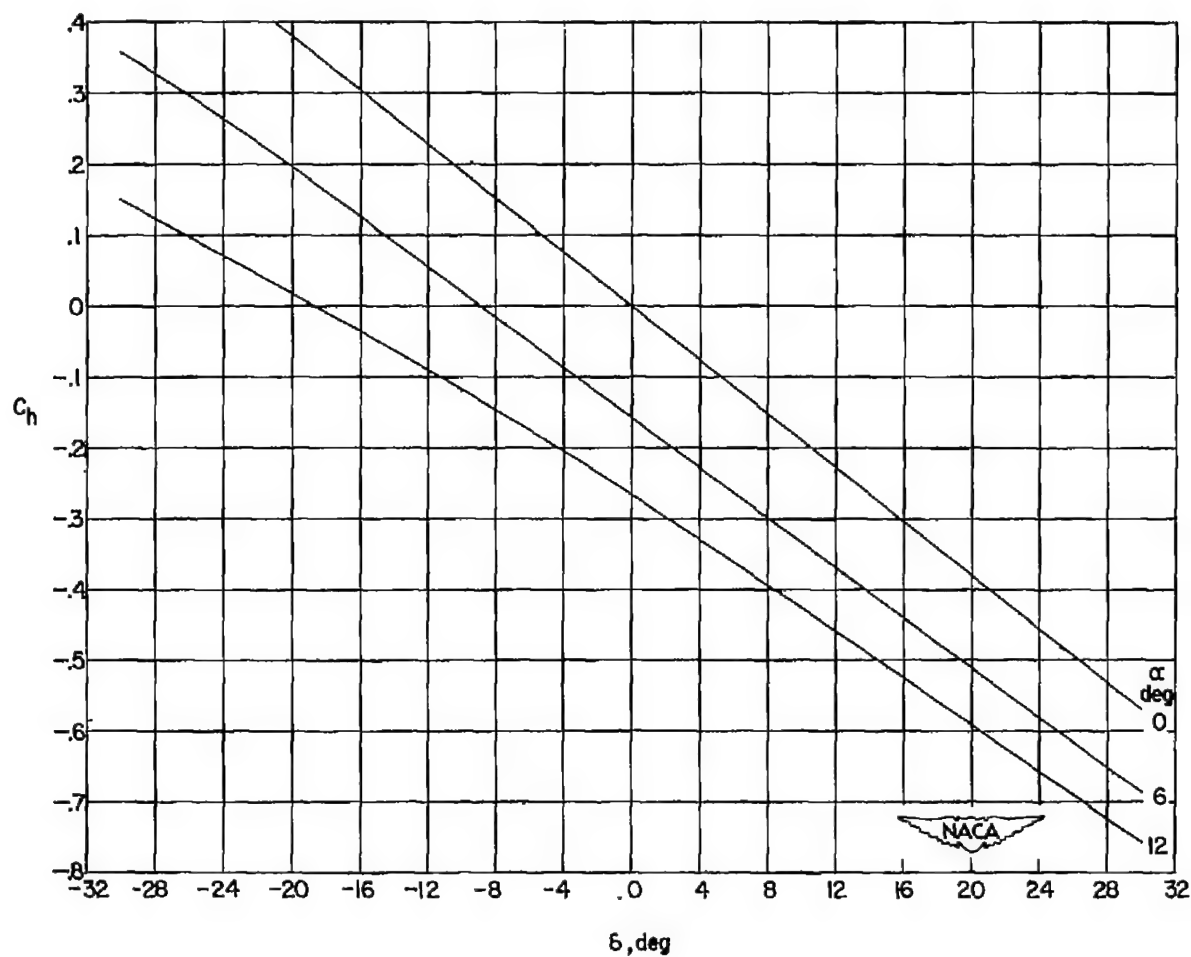
NACA
L-77038

~~CONFIDENTIAL~~

NACA RM 152K28

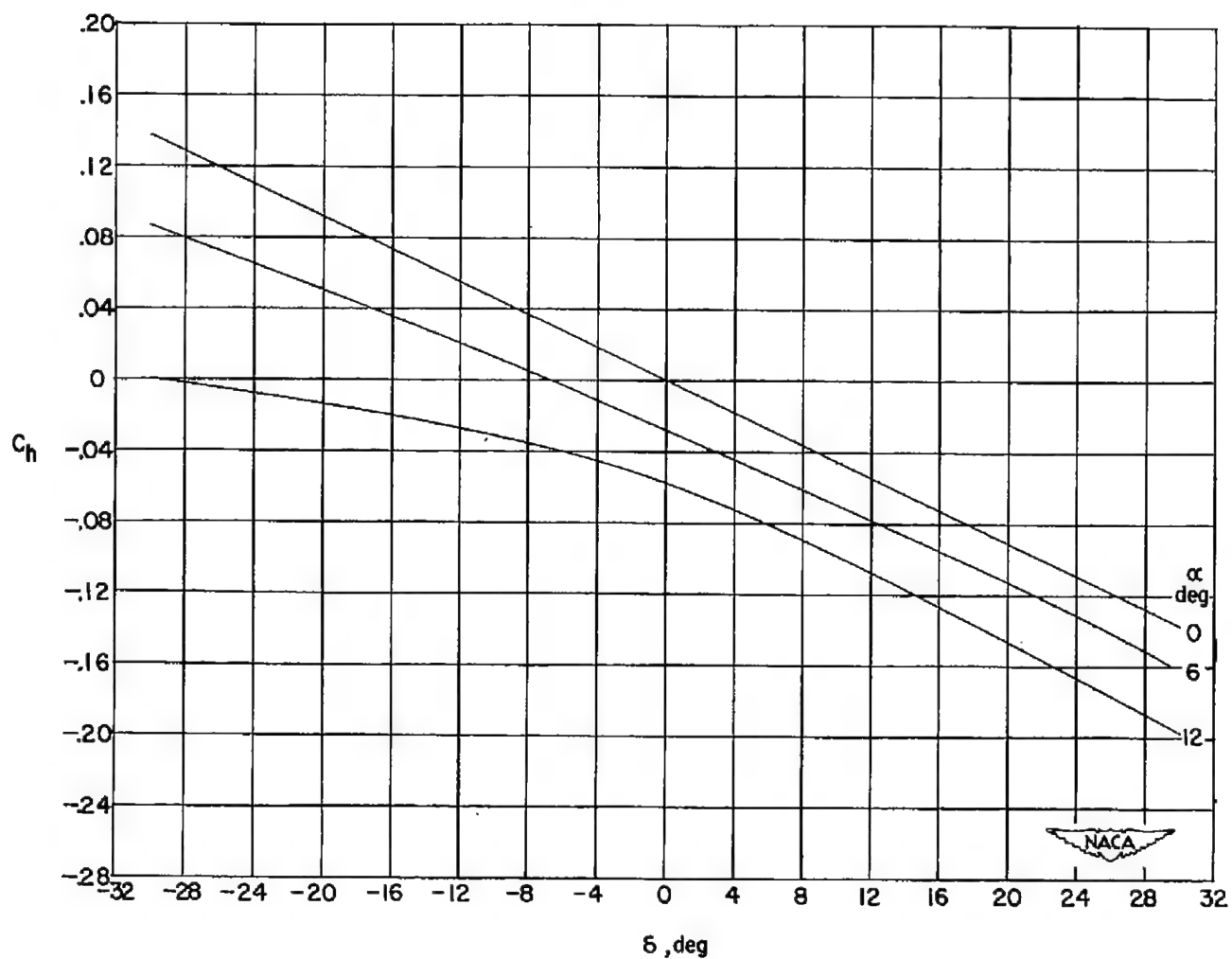


Figure 4.- Half-span delta-wing model installed on boundary-layer bypass plate. (Flap illustrated not used in this investigation.)



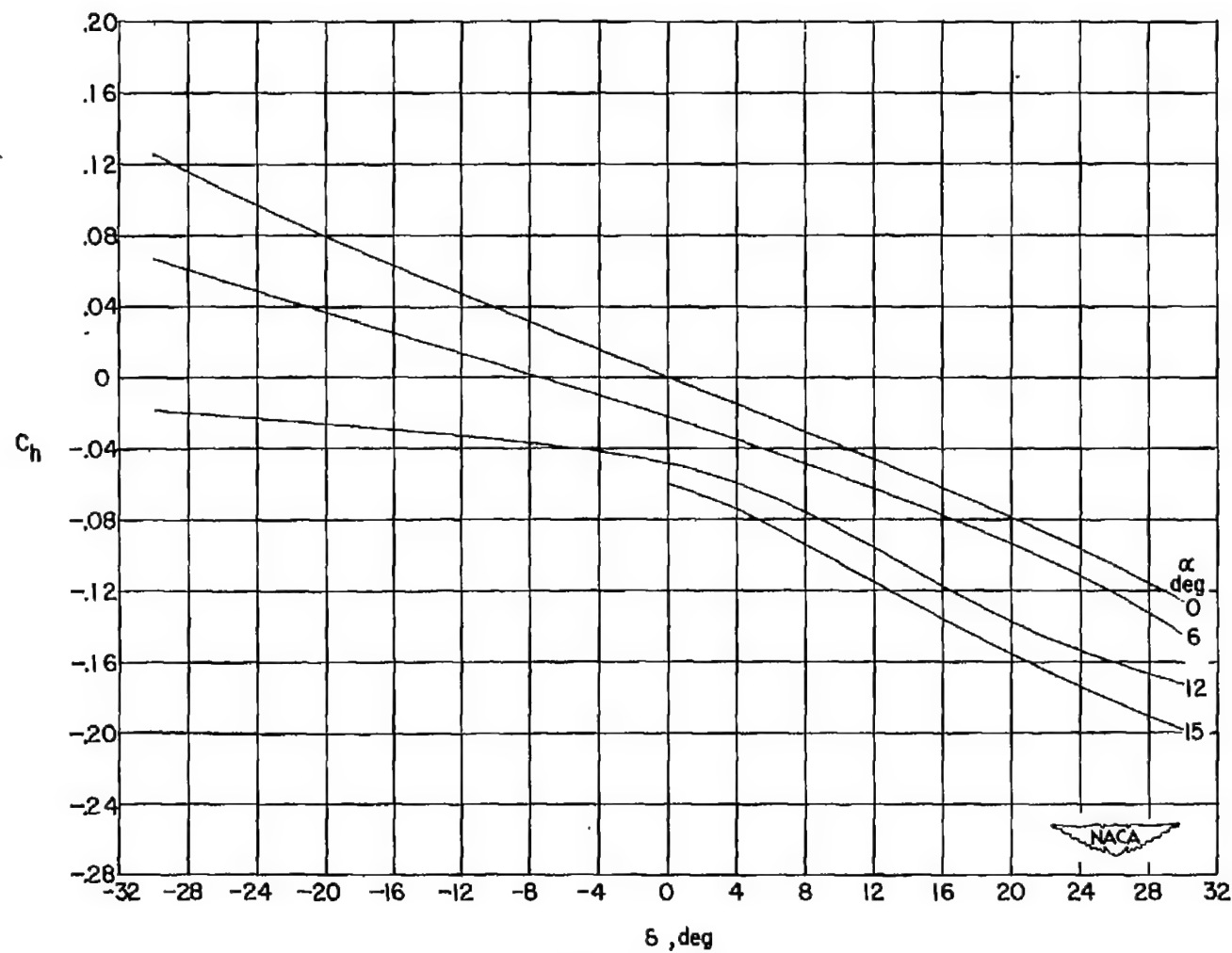
(a) Configuration A.

Figure 5.- Variation of control-surface hinge-moment coefficient with control deflection.



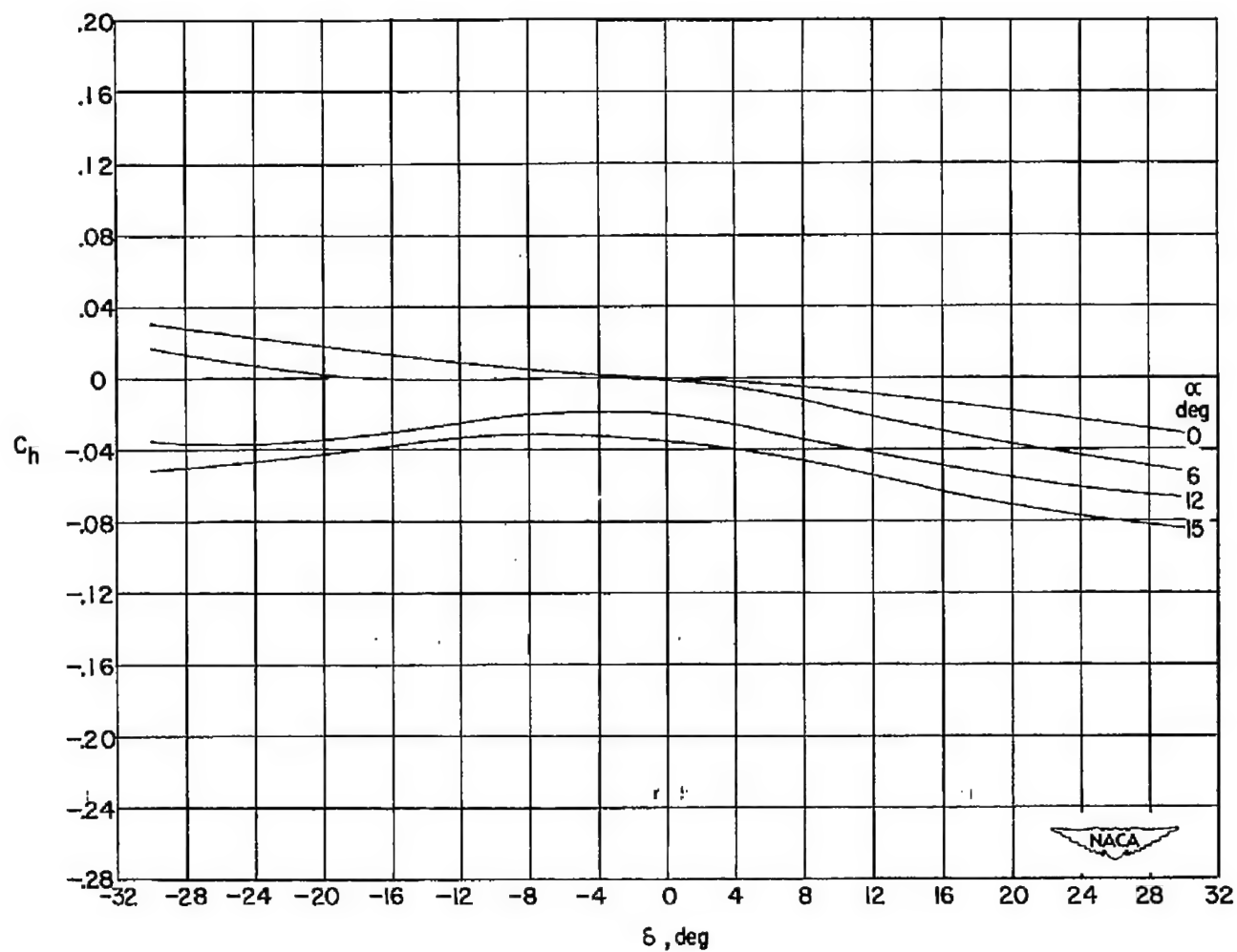
(b) Configuration B.

Figure 5.- Continued.



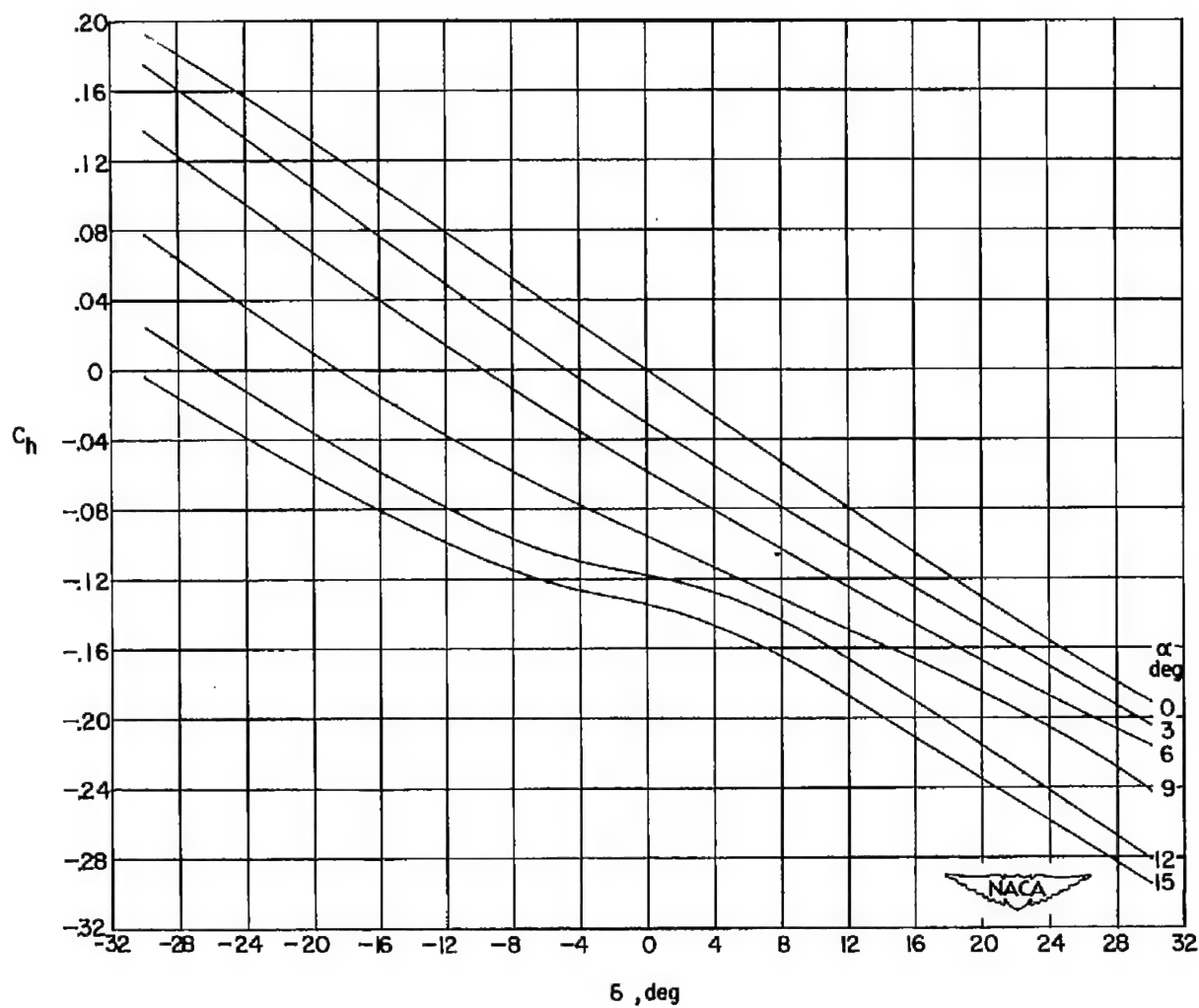
(c) Configuration C.

Figure 5.- Continued.



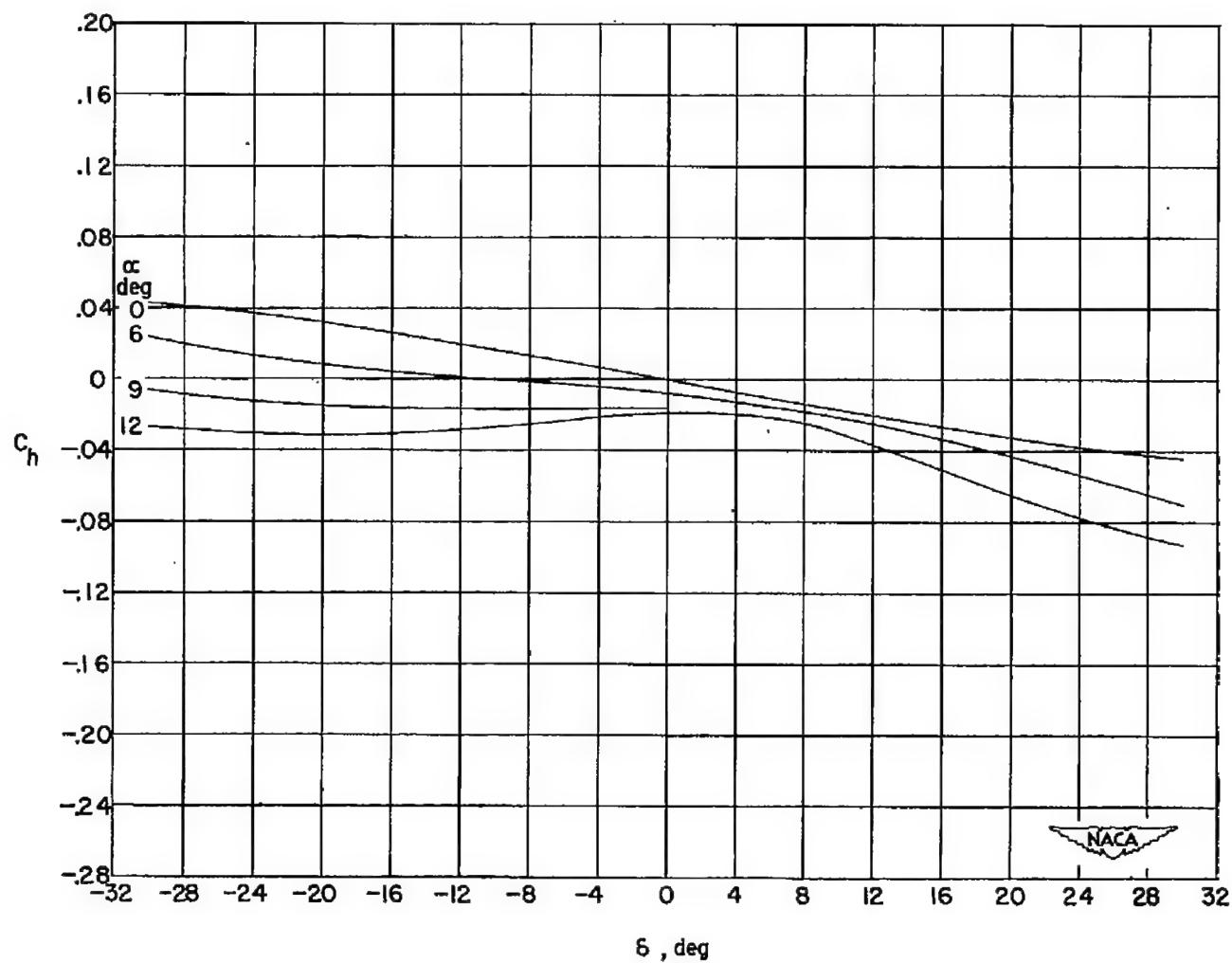
(d) Configuration D.

Figure 5.- Continued.



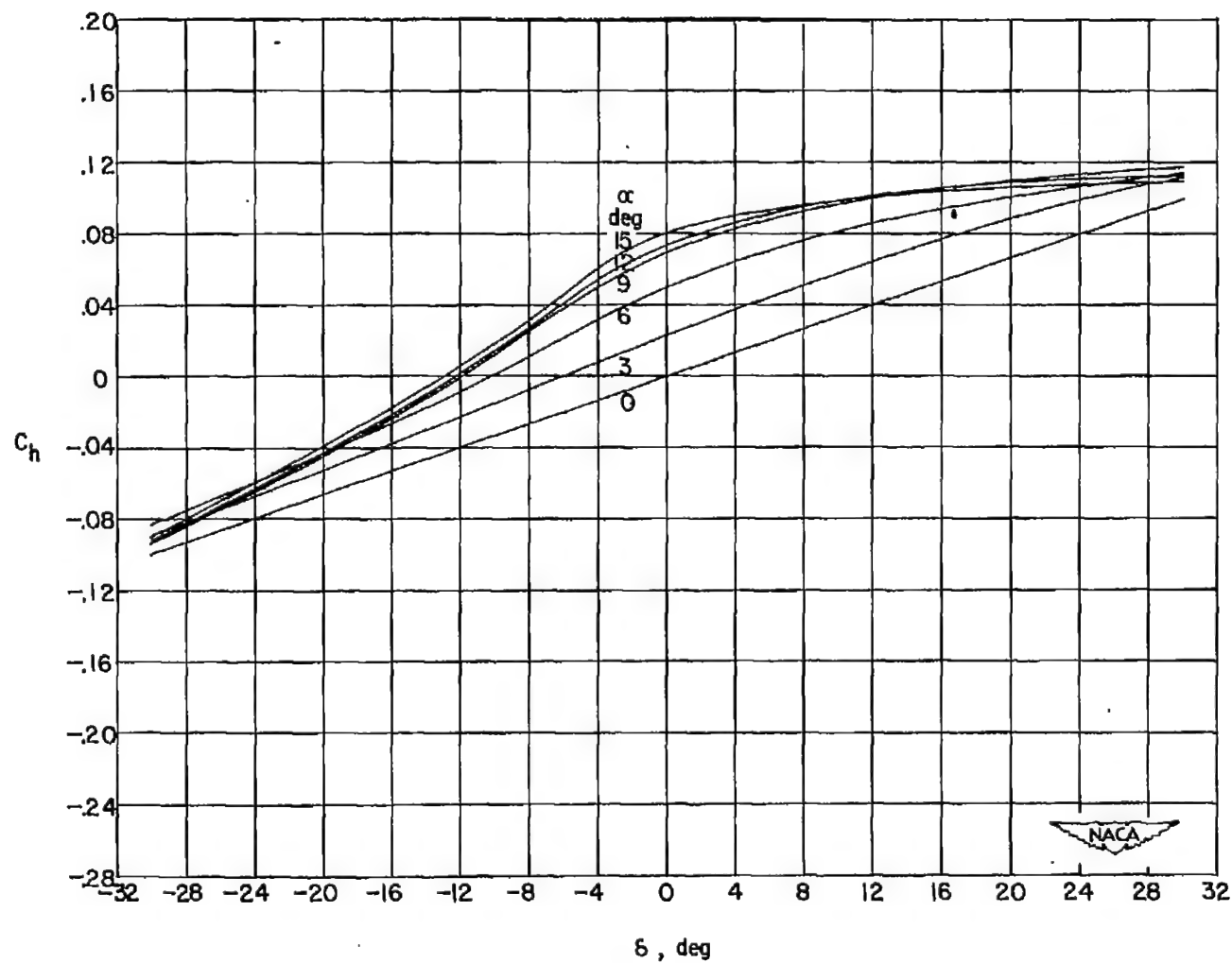
(e) Configuration E.

Figure 5.- Continued.



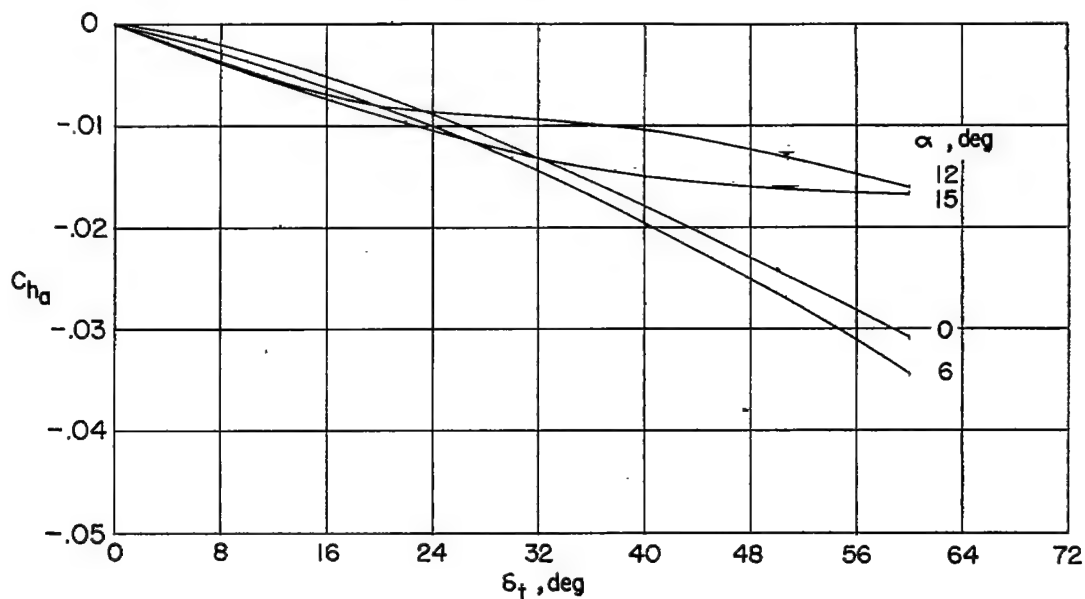
(f) Configuration F.

Figure 5.- Continued.

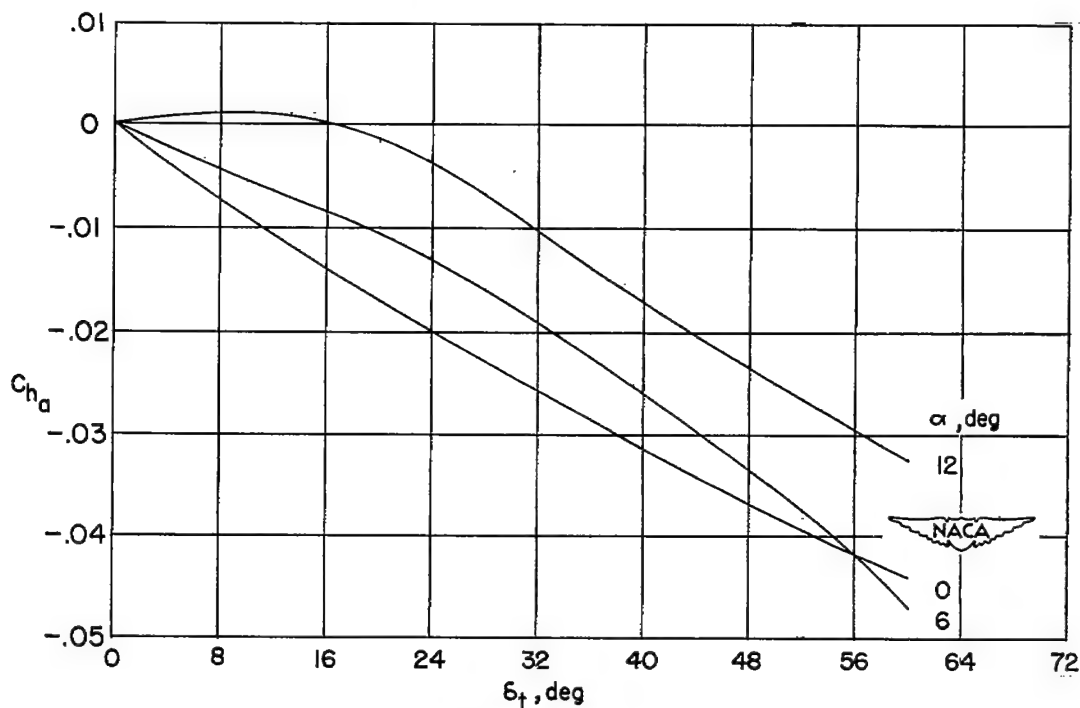


(g) Configuration G.

Figure 5.- Concluded.

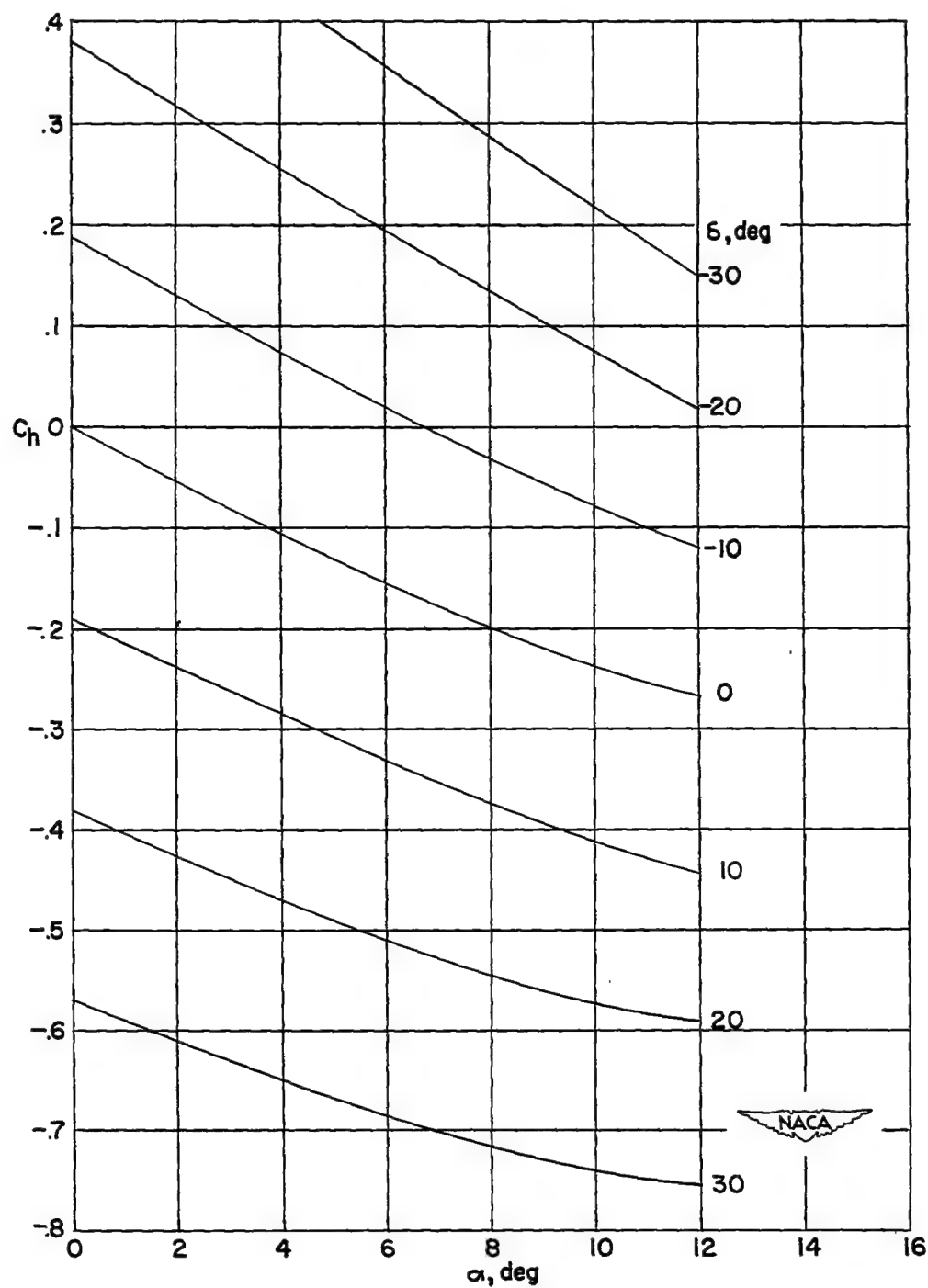


(a) Configuration D.



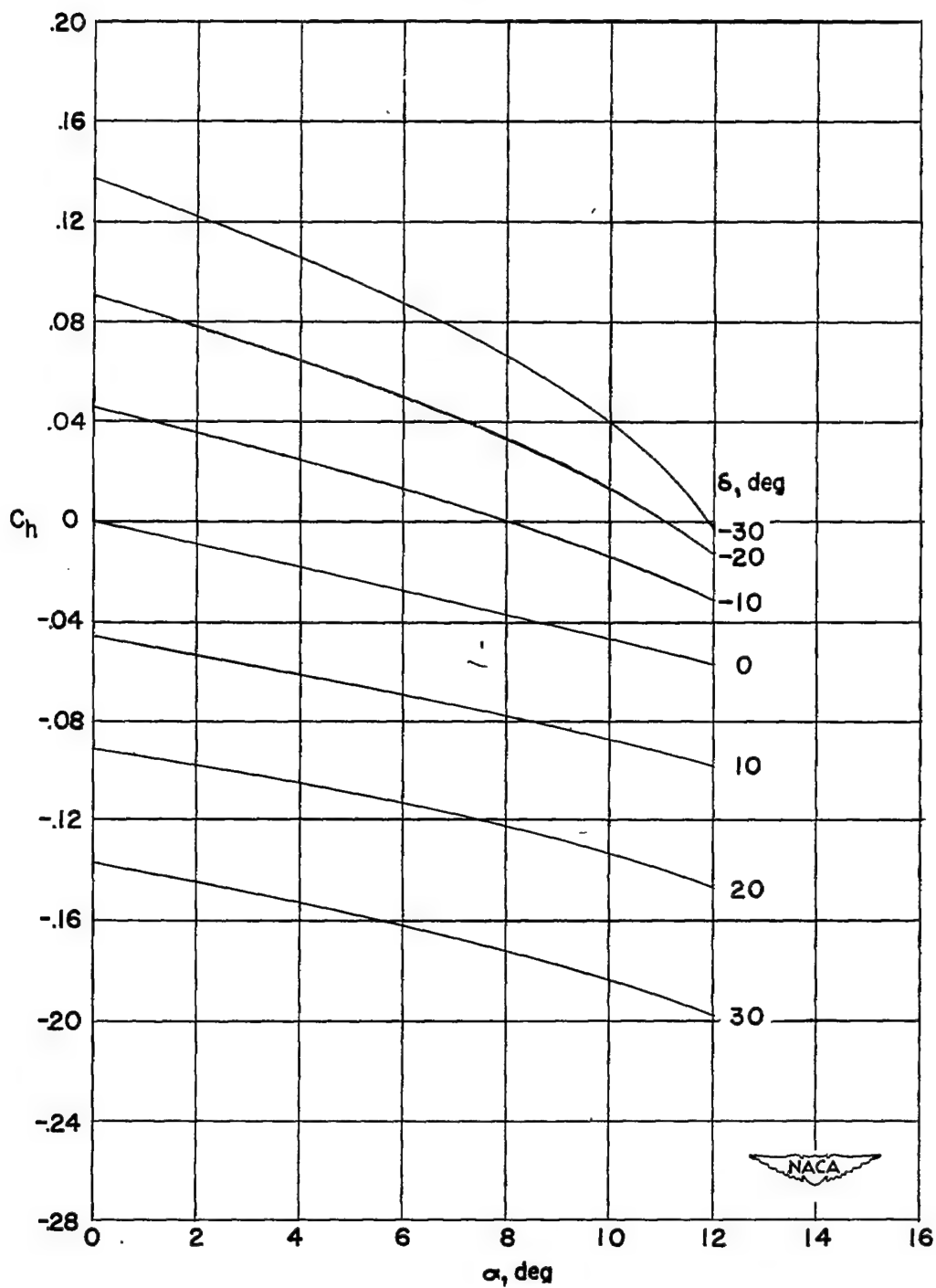
(b) Configuration F.

Figure 6.- Variation of net control-surface hinge-moment coefficient with total control deflection for two controls deflected as ailerons.



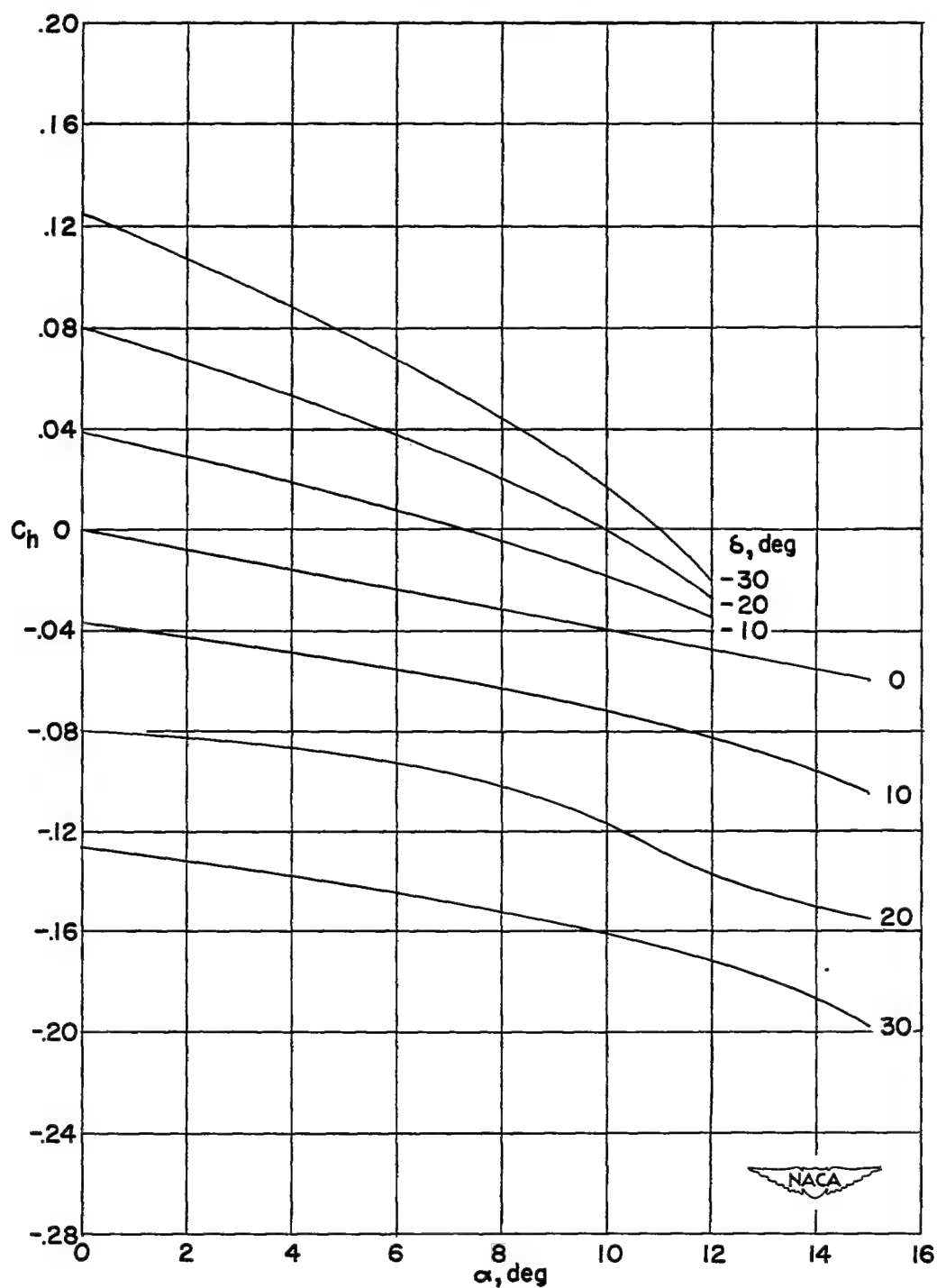
(a) Configuration A.

Figure 7.- Variation of control-surface hinge-moment coefficient with angle of attack.



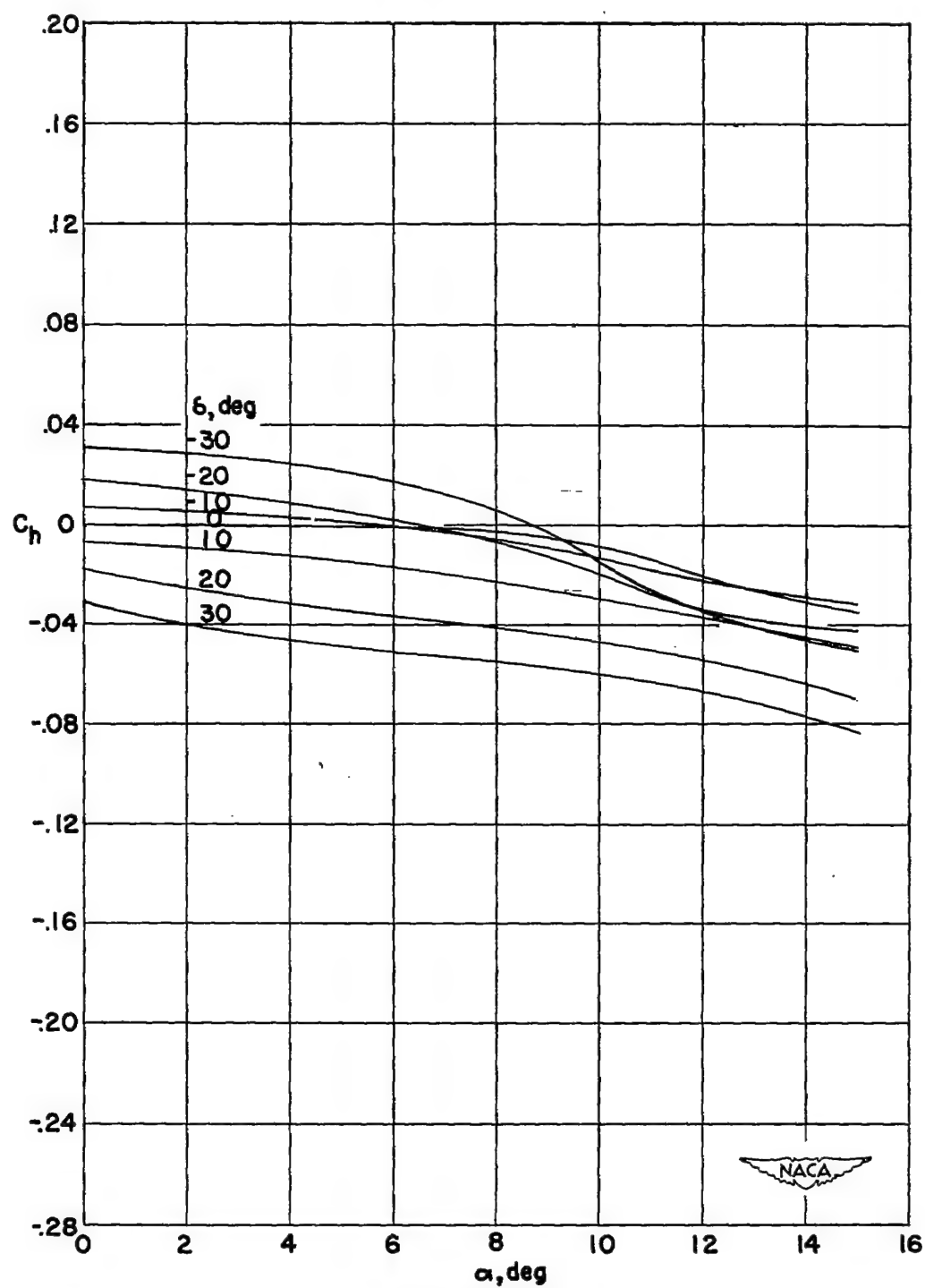
(b) Configuration B.

Figure 7.- Continued.



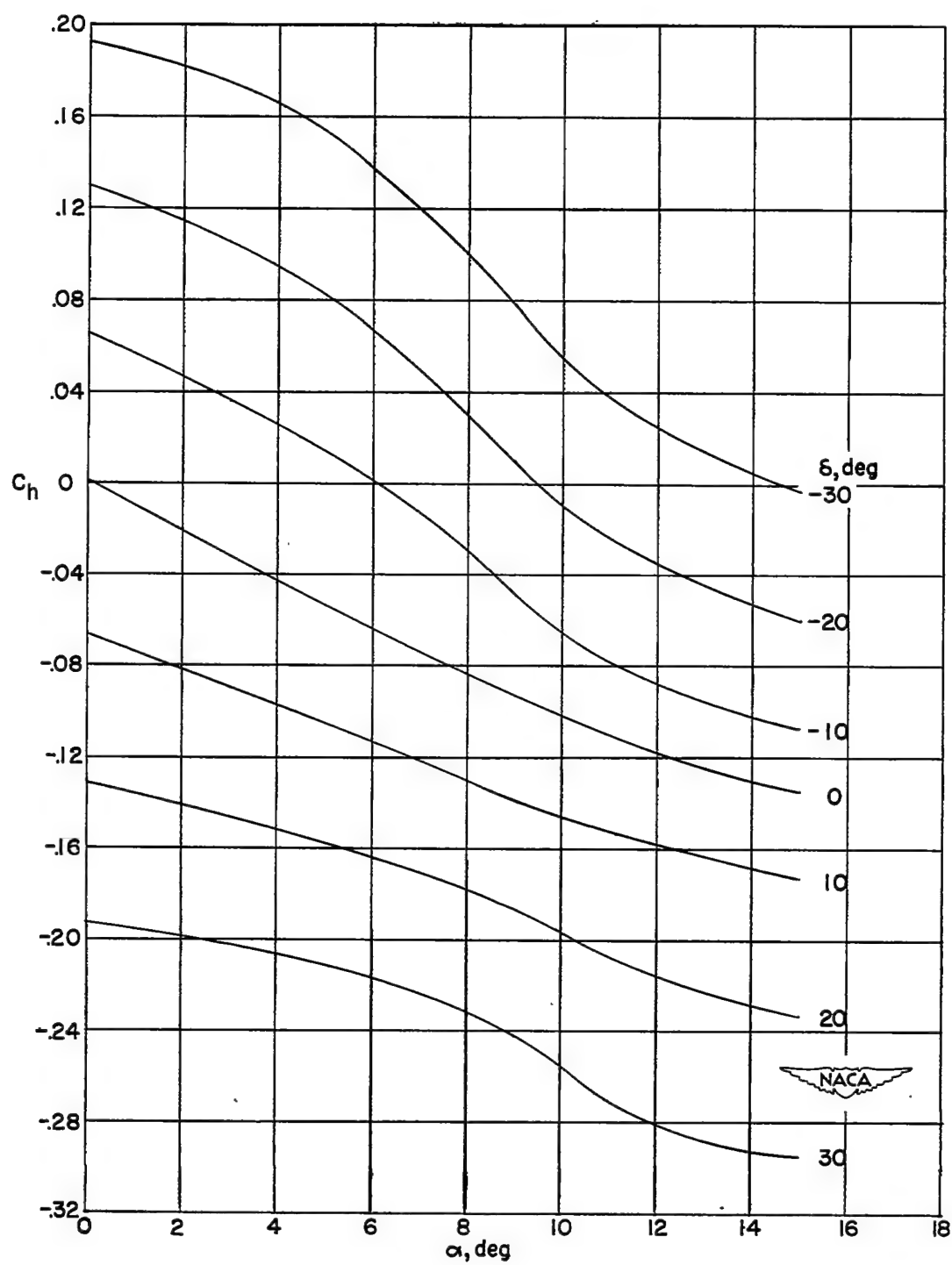
(c) Configuration C.

Figure 7.- Continued.



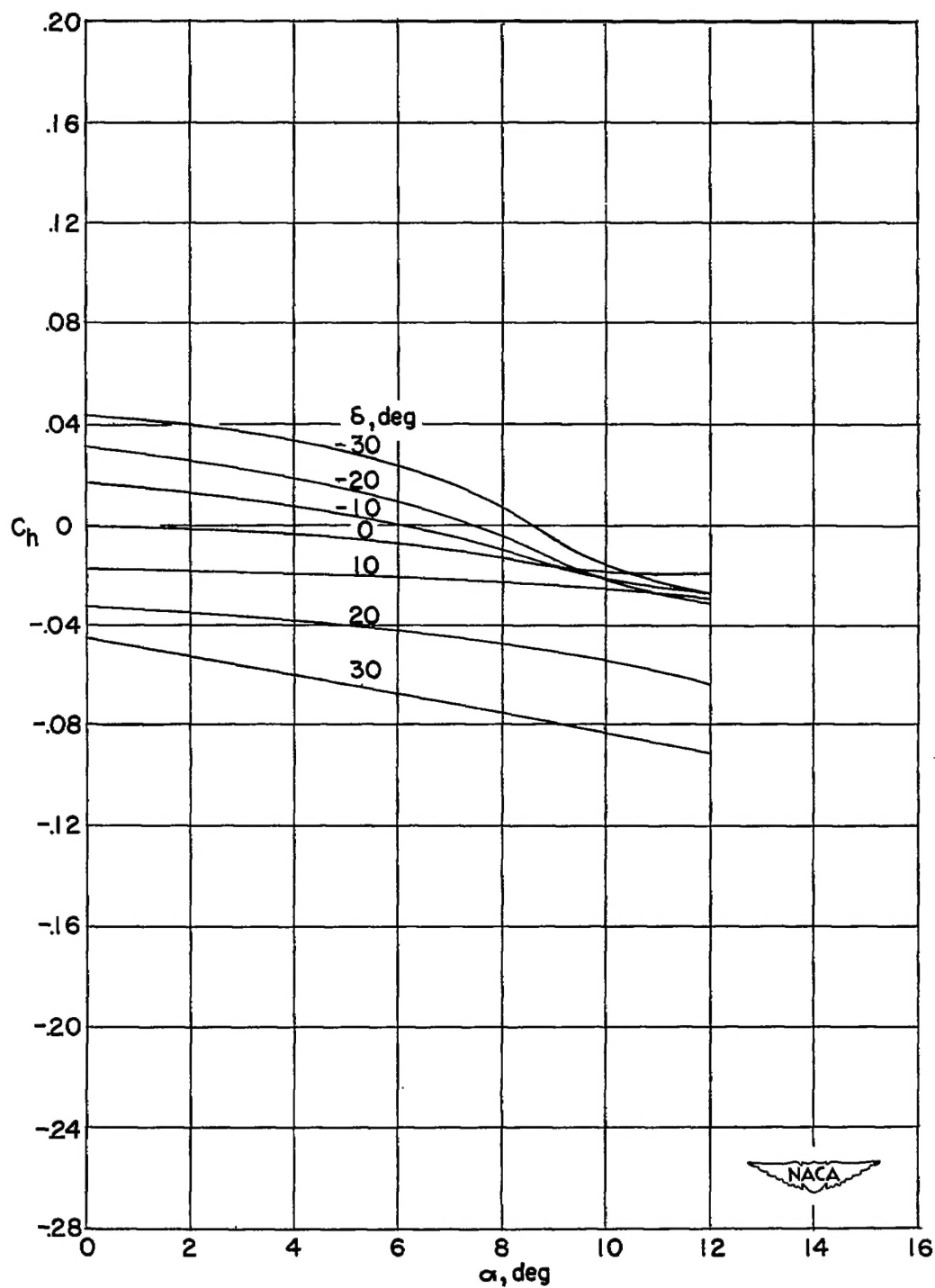
(d) Configuration D.

Figure 7.- Continued.



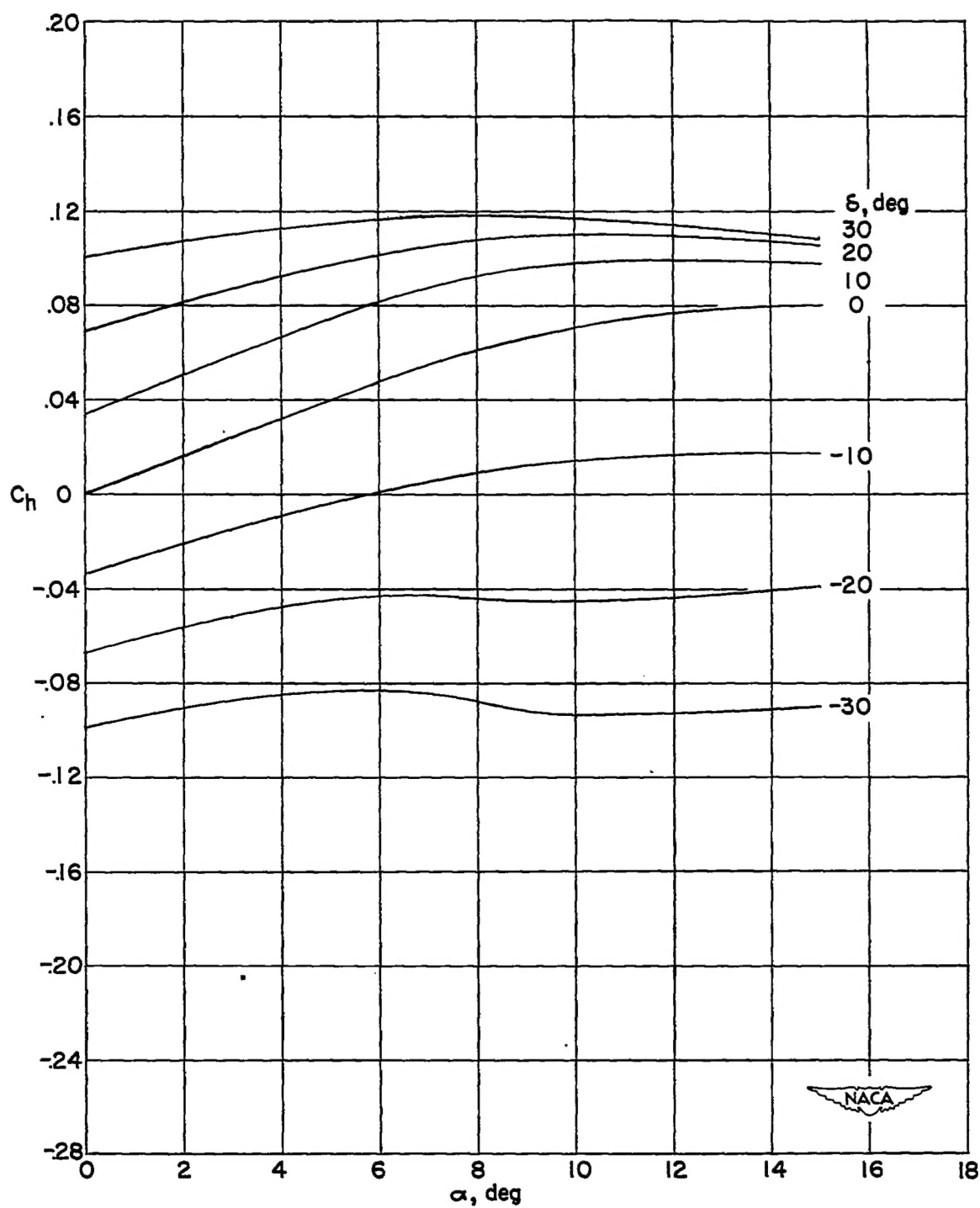
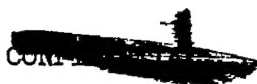
(e) Configuration E.

Figure 7.- Continued.



(f) Configuration F.

Figure 7.- Continued.



(g) Configuration G.

Figure 7.- Concluded.



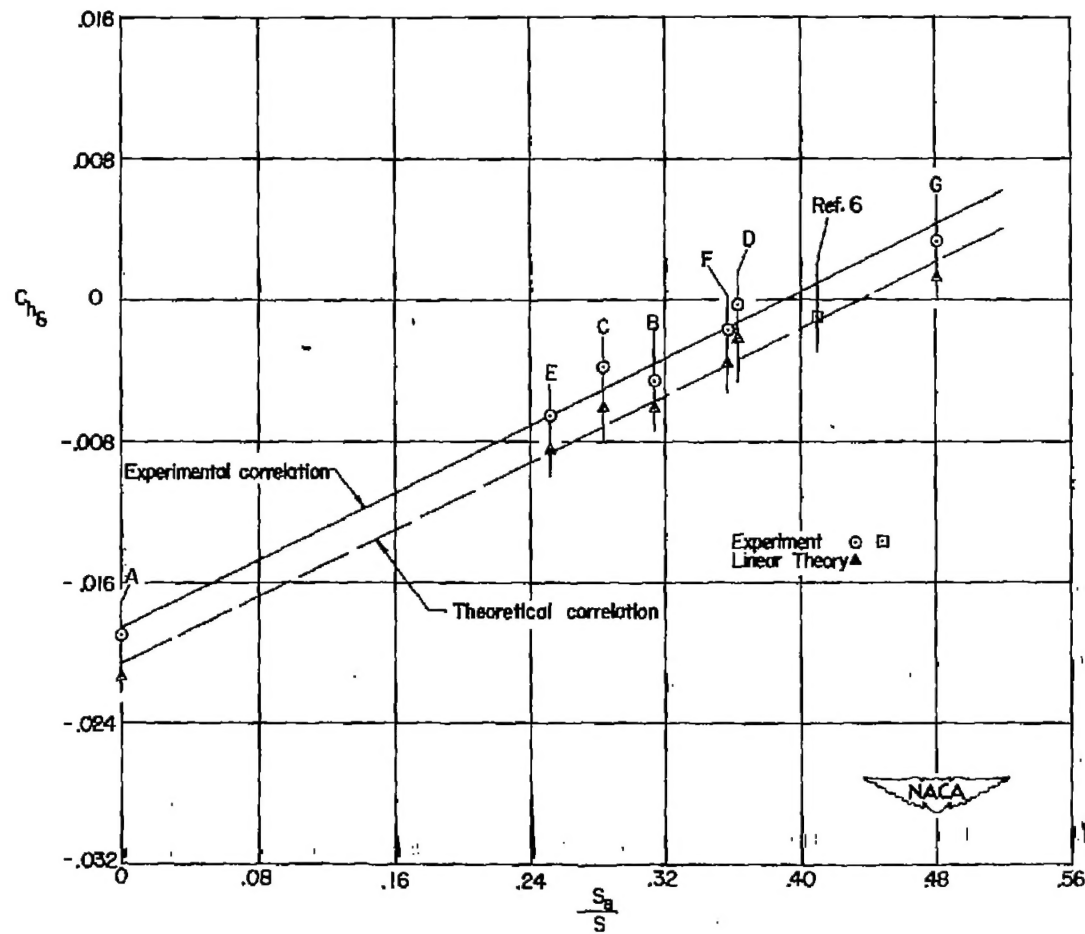
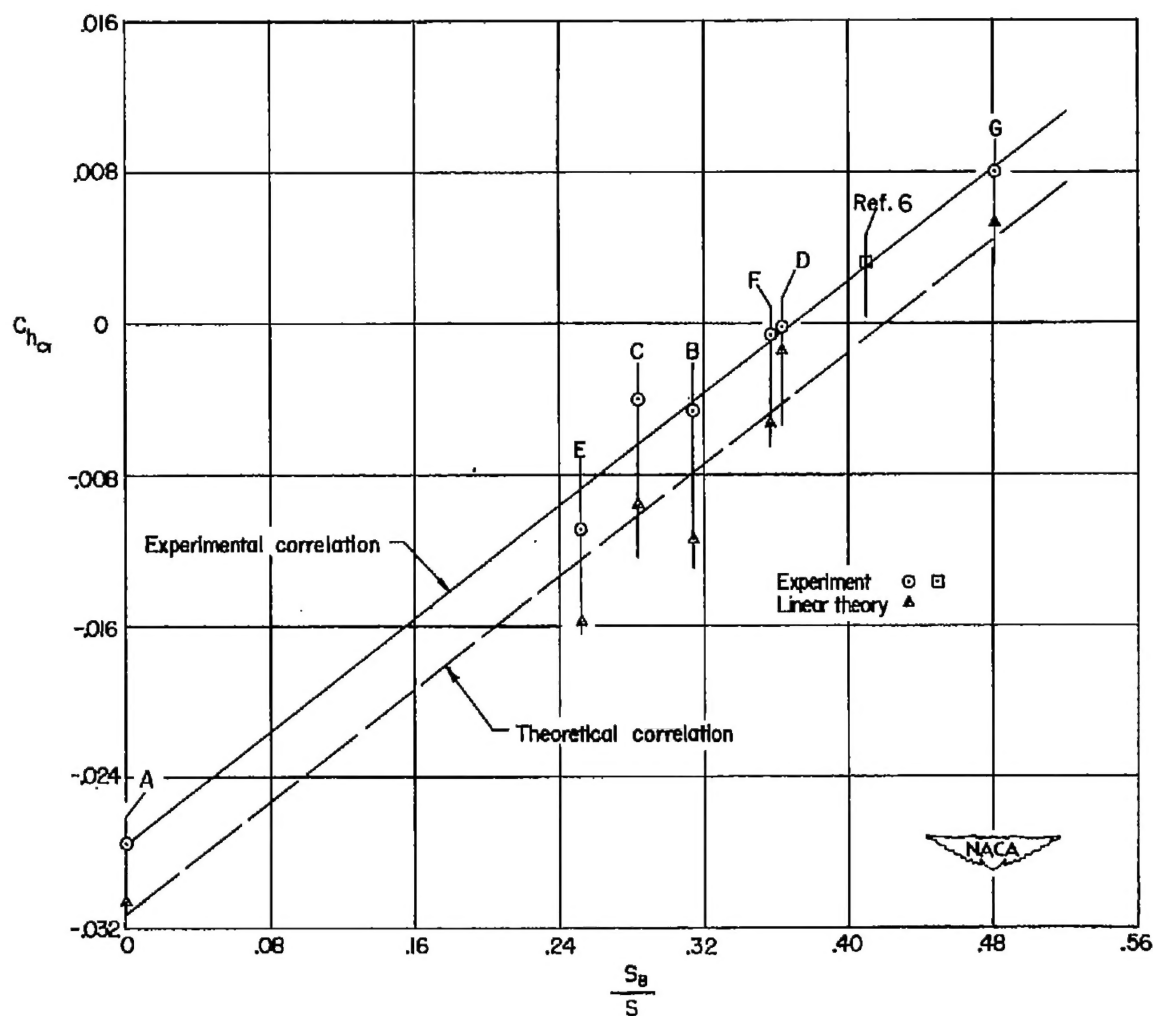
(a) C_{h8} .

Figure 8.- Variation of theoretical and experimental hinge-moment-coefficient parameters C_{h8} and $C_{h\alpha}$ with balance-area to total-control-surface-area ratio. Letters identify configuration.



(b) $C_{h\alpha}$.

Figure 8.- Concluded.